



AMERICAN METEOROLOGICAL SOCIETY

Bulletin of the American Meteorological Society

EARLY ONLINE RELEASE

This is a preliminary PDF of the author-produced manuscript that has been peer-reviewed and accepted for publication. Since it is being posted so soon after acceptance, it has not yet been copyedited, formatted, or processed by AMS Publications. This preliminary version of the manuscript may be downloaded, distributed, and cited, but please be aware that there will be visual differences and possibly some content differences between this version and the final published version.

The DOI for this manuscript is doi: 10.1175/BAMS-D-11-00163.1

The final published version of this manuscript will replace the preliminary version at the above DOI once it is available.



4

8

The lifecycle of a radiosonde

12

FEDERICO FLORES, ROBERTO RONDANELLI*

Department of Geophysics, University of Chile

16

MARCOS DÍAZ, RICHARD QUEREL, KAREL MUNDNICH,

LUIS ALBERTO HERRERA, DANIEL POLA, TOMÁS CARRICAJO

20

Department of Electrical Engineering, University of Chile

24

28

32

36

40

44

48

52

56

60 *Corresponding author address: Roberto Rondanelli, Department of Geophysics, University of Chile Santiago, Chile
E-mail: ronda@dgf.uchile.cl

Abstract

64 The development of scientific instruments was, only a few years ago, confined to universities and
electronic companies having highly specialized human and/or technical resources. With the advent of
open hardware initiatives, engineers, scientists, hobbyists and even people with limited electronic skills
68 have been able to tinker with complex electronic systems. Taking advantage of these inexpensive and
widely available tools and in the context of an engineering project class for under-graduates, we set
about building a working radiosonde prototype from the ground up, based on an open hardware platform
and easily accessible components.

72 As a result, we have built a fully functional radiosonde that measures, records and transmits pressure,
temperature, humidity and wind, plus a small camera that stores images on to a flash card. A release
system was also developed so that the radiosonde can be detached from a balloon upon reaching a
76 certain height, pressure level or flight time. Once released, one can attempt the recovery of the
radiosonde with the help of a pre-calculated trajectory using a numerical mesoscale forecasting model
and visualization software. We compared the performance of our sonde with two commercial
radiosondes using climate chambers and two field launches. We will also discuss some of the more
80 interesting capabilities we foresee for such a platform: 1) collaboration between meteorology and
engineering departments in both education as well as research, 2) development of a flexible hardware
platform that allows for an effective way to compare different commercially available sensors and to
easily integrate new prototype sensors.

84

1. Introduction

88

The importance of the radiosonde as a tool for gathering meteorological data is enormous. The radiosonde allows in a matter of minutes and at relatively low cost, measurement and transmission of data from regions mostly inaccessible to humans. Key advantages of the radiosonde over other observing systems are its relatively low cost, high accuracy and high vertical resolution in-situ vertical profiles of the atmosphere from the surface up to tens of kilometers. The development of the first radiosondes around 1924-1931 (see historical discussions on priority and first publication of radiosonde data in DuBois et al. (2002) and Pettifer (2009)) paved the way for numerical weather forecasting as well as allowed researchers to test the theoretical foundations of dynamical meteorology. Much of what we know about the atmosphere comes from data originally measured and transmitted by one of these instruments, so it is no exaggeration to call the radiosonde the fundamental instrument in meteorological research. Although satellites have filled much of the gaps in our knowledge of the upper atmosphere, there is still the need for radiosondes to provide high quality and high resolution data not only for calibration of other observing systems, but also for basic meteorological research, for creating the analyses needed to initialize weather forecasting models and for detecting climate trends.

104

Current radiosondes have evolved into a relatively standard and well developed set of instruments that measures temperature, pressure and humidity. Wind is currently inferred from the GPS position of the radiosonde assuming that the carrying balloon acts as a passive tracer with respect to horizontal winds and filtering the pendular motion of the radiosonde package. Several technological improvements of the radiosonde have been led by the Finnish company Vaisala (especially since the 1980s) which produced about 70% of the radiosondes used globally by 2002 (Dabberdt et al. 2002). The World Meteorological Organization has established requirements for the accuracy of the data gathered by a radiosonde (see e.g. Nash et al. 2011). For instance, operational standards allow for errors of 1 K in the tropospheric temperature and less than 7.5% in the relative humidity. Operational standards are still too

112

relaxed when compared, for instance, to the magnitude of the climate trends that we expect to detect from the observational record over a period of decades (observed trends in midtropospheric temperature during the last 30 years range from about -0.1 K/decade to 0.2 K/decade (Thorne et al. 2011)).

116 Therefore, more stringent requirements are being proposed for climate monitoring that allow for errors of less than 0.3 K in temperature and less than 3% relative humidity in the troposphere (Immler et al. 2010; Nash et al. 2011). Humidity measurements also suffer from low accuracy in the upper troposphere and stratosphere (Miloshevich et al. 2009), regions which provide only a small fraction of the total water

120 vapor in the atmosphere, but that have a significant impact in the radiative transfer of longwave radiation.

Only about 1000 synoptic radiosonde stations exist around the globe. This is explained by the

124 relatively large operational cost of the ground stations, including the cost of the receiving station, the gas supply, the radiosondes and the personnel in charge (see e.g. Douglas 2010). Receiving stations are usually up to 100K US\$ (or at the lower end, 5K US\$ for InterMet boundary layer systems that consists mostly of a radio receiver, a modem interface and the software). Each individual radiosonde costs about

128 200 US\$. The cost of establishing a radiosonde ground station makes it difficult to increase the spatial extent of the radiosonde network, which is particularly deficient in vast regions of the Southern Hemisphere.

132 Given the relevance of this instrument for research as well as day-to-day operations in forecast centers (weather and air pollution), airports, and other applications, and the availability of inexpensive micro-controllers and sensors, we challenged ourselves to build a radiosonde with commercial off-the-shelf parts and materials within a semester and within reasonable budget constraints. It is fair to ask the

136 question: Why bother reproducing an already well developed meteorological instrument? The main purpose of our exercise was pedagogical, so even if the radiosonde turned out to be more expensive than a commercial one, there would still be a value in developing it as an engineering project. Besides the purely pedagogical value of the exercise, building an “open hardware” radiosonde allows for the

140 accelerated development by a community of users. Also, we envisioned the prototype of our sonde as a standard platform that could be easily adapted and used by the global community. The possibility of

adding and comparing different sensors can potentially lead to improvements in the accuracy, price, weight, and durability of sensors, batteries, actuators and other components.

144

We are aware of the existence of projects that bear some similarities to the one we present here. On one side of the spectrum, there are several hobby-oriented projects whose main objective is usually to get images and recordings from the upper atmosphere and usually attempt the recovery of the payload. On the other side, there are several research-oriented projects usually carried out by large labs and they involve the design of specific soundings focusing on a particular research objective. Our project differs from purely hobby-oriented projects in that we attempt to obtain high quality data; on the other hand our project differs from purely research-oriented projects in that we have a strong pedagogical component. Our project also differs from a commercial radiosonde in that we attempt our project to be completely “open” in both hardware and software platforms, so it can be easily replicated and improved.

148

152

156

In the next section we will briefly describe the logistics of the classwork as well as the hardware and software used for building the radiosonde and programming the micro-controllers as well as the graphical interface of the sounding ground station. In Section 3 we describe some of the tests carried out using our instrument. In Section 4 we ask the question of whether the engineering students learn any meteorology during the building and operation of the radiosonde. Finally in Section 5 we discuss some possible uses and improvements of the radiosonde platform.

160

164 2. Building the radiosonde

168

a. Research and development teams

In the context of a second year engineering class called Engineering Project Workshop at the University of Chile, the students are asked to “conceive, design, implement and operate an engineering project, that gives an innovative solution to a problem in a specific area” (inspired in the so-called CDIO approach (Crawley et al. 2007)). As other meteorology groups around the world, our Geophysics Department is embedded within an engineering school. Many of the faculty in the meteorology group

172

had a background in engineering before moving into the atmospheric sciences, and are usually asked to
176 teach sciences to the engineering students. As an applied science, problems in meteorology usually offer
a variety of challenges for almost all specialties within a classical engineering school. Therefore,
meteorology offers the potential of providing design problems that are interesting for engineering
faculty as well as for a large number of students with a breadth of different interests and backgrounds.
180 We believe that the building of a radiosonde is one of such problems.

We will illustrate this by enumerating some of the challenges the students faced during the process
of building a radiosonde. Some of these issues are usually covered in the typical curriculum of
184 engineering as purely theoretical problems, for instance, when studying viscous dissipation in a fluid
students may be asked to calculate the terminal velocity of a balloon filled with a gas lighter than air, or
in chemistry students may be asked to find the equilibrium water vapor pressure of a given solution at a
certain temperature and pressure. These are usually unrelated problems, given in the context of a set of
188 sequential classes in the basic and applied sciences. There is a more meaningful and deep learning when
these problems appear not in isolation, and perhaps even more important, when the resolution of the
individual problems is critical for the successful completion of the project. In Table 1, we show an
example of some of these tasks and we have loosely identified them with some engineering specialty.
192 Most of the activities shown in the table were effectively carried out during the semester.

At the beginning of the 15 week semester, we proposed the problem to the 15 students taking the
class and initially motivated them about the possible applications of such an instrument. We had the help
196 of 6 teaching assistants (4 students from electrical engineering and 2 students from meteorology). The
class was divided into 3 groups each composed of 5 students and 2 research assistants and we gave each
group a different task: temperature-humidity measurement, pressure-wind measurement and radio
communications. As the semester advanced, the three groups of students specialized into their
200 designated tasks and were required to interact with the other groups in anticipation of the final
integration of the radiosonde components. The student groups suggested two additional features that
would distinguish their unit from a commercial radiosonde: 1) a camera to record images during the
flight, and 2) a release system so that the sonde could be detached from the balloon during the flight and
204 potentially be recovered.

b. Hardware

208 The computational core of the radiosonde is an Arduino board, an open-source electronics
prototyping platform (<http://arduino.cc/>). Arduino was selected because it provides a complete, flexible,
easy-to-use hardware and software platform that is widely used not only by engineers, but also by artists,
212 designers, and hobbyists (e.g. Sarik and Kymissis 2010). The sensors, GPS, transceiver, release-linear-
motor, memory card and camera in the radiosonde are connected to the Arduino via a customized
daughter board, or “shield” in Arduino nomenclature. The ground receiver consists of an Arduino and a
transceiver module which are easily connected to a computer where data is stored. Pictures taken by the
216 radiosonde camera are stored internally on the memory card and not transmitted due to bandwidth
limitations. Fig.1 shows a view of the components as they were laid out in our final prototype.

The radiosonde and receiver hardware used in our tests were based on the version of the Arduino
220 board called “Arduino Duemilanove”. Recently, the source code has been updated to also work with
newer versions of the Arduino board: the “Arduino Uno” and “Arduino Mini Pro”). The choice of
original sensors was made by students in consultation with the teaching assistants and professors. When
deciding on sensors we attempted to obtain those that were inexpensive but that could also provide high
224 quality meteorological data. Table 2 shows a description of the sensors used in building the radiosonde.
More detailed specifications of the sensors, parts and their connections to the Arduino board, as well as
circuit diagrams are available at <http://www.dgf.uchile.cl/radiosonde>

228 *c. Software*

A summary of the information flow from the radiosonde is as follows: raw data (voltages) are
232 measured by the sensor/transmitter unit and communicated to the receiver unit which is connected to a
computer where the voltages are converted to actual meteorological values. The radiosonde software is
divided into three distinct programs: Arduino instructions for the transmitter/sensor unit, Arduino
instructions for the receiver, and a computer-based GUI interface to process and display the received

236 data.

The Arduino instruction sets are compiled and uploaded to the Arduino boards using a command-line interface and MAKE file. The rather simplistic Arduino integrated development environment was not used since some compilation errors would occur when certain external C++ libraries were included.

The computer-based GUI, called BaseCamp, has been compiled and run on Windows, Linux and OSX systems (see screenshot in Figure 2). All programs and source code will be available for download from the radiosonde project website.

244

3. Calibration and cross-comparison

248

a. Preliminary experiments

252 We performed several test experiments in preparation for the main field launch. A tethered balloon campaign was conducted at the end of the semester activity where the radiosonde was first used to transmit meteorological data from an altitude of about 1000 m above ground level. We also tested the data-link from the transmitter to the receiver by communicating between the top of Cerro San Cristobel (850 m.a.s.l) and the top of the Geophysics Department building in Santiago (520 m.a.s.l) about 4 km line-of-sight with an unobstructed view of the hill. A successful transmission of meteorological data was completed including GPS data as shown by the trajectory of the team carrying the sonde as they were climbing up the hill in Figure 2. We also performed a second communication test where successful transmission was established from a park near the Andes piedmont and the top of the Geophysics building, about 13 km line-of sight.

260

b. Methodology for release and recovery

264

Besides being able to compare data measured with our sonde with those obtained with the research-grade radiosondes, we tested the possibility of recovering the equipment. While the notion of recovery was at first a curiosity, it quickly became an important objective of the campaign as the team grew attached to the product of several months of work. Recovery of balloon-borne equipment was an

268

essential part of the early attempts to characterize the upper atmosphere. Those balloonsondes only carried registering apparatus and therefore needed to be recovered in order to retrieve the data. For instance, the discovery of the tropopause in 1902 was made using these balloonsondes by Teisserenc de Bort (1902) and Assman (1902) (see e.g. DuBois et al. 2002).

In order to recover the radiosonde, we took advantage of three features of our sonde, two of them not available to the early balloonists. First, the release system was able to detach a balloon from the sonde at any given pressure level, upon reaching a certain temperature or elapsed flight time, allowing the sonde to travel a pre-determined distance in the vertical. Second, the GPS signals from our sonde and one of the commercial sondes, allowed us to accurately know their positions. Third, we made use of a WRF (Weather Research Forecasting Model, Skamarock et al. (2008)) forecast simulation with a resolution of ~ 6 km in the horizontal and 50 eta levels in the vertical, with 10 eta levels located lower than 0.9 with a top pressure of 50 hPa. The model forecast winds were used to determine the sonde trajectory, allowing a recovery team to be ready near the projected landing zone. Reviewing the literature we learned that the recovery system devised by the students was not new and was originally called the “multiple balloon technique” reported by Hugo Hergesell in 1904 (Hergesell 1906; DuBois et al. 2002). Our technique and the original one were effectively the same: two balloons would produce the lift necessary for an ascent of ~ 5 m/s of the payload (three sondes weighting in total 1250 g) and in our case, at a given pressure level the linear actuator would release one of the balloons so that the remaining one would carry the payload back to the ground at ~ 2 m/s of vertical descent velocity. In the accounts given by the early balloonsonde researchers, they report high rates of recovery based mostly on the willingness of countryside people to return the equipment in exchange for a reward (see for instance Clayton and Fergusson (1909)). In our case, evidence from comparing WRF-forecast and real sonde trajectories showed that the trajectories were sufficiently close to the real trajectories (especially for the region below 10 km height and within the bounds of the city) so as to allow a recovery team to be within the range of the radiosonde signals at ground level (much smaller than the range of the reception of the sonde in flight), and perhaps, even observe the descent of the sonde (see Fig. 3). The multiple balloon technique has an additional advantage over the most common approach/technique of using a parachute; if the line attaching the payload to the descent balloons is given sufficient length, it will serve as a

marker for the position of the radiosonde package. This was successfully tested by Hergesell (1906) over the ocean.

300

c. Boundary layer sounding

304

Our first field experiment was designed to test all sensors in a real flight that included ascent and descent. The flight was launched on October 1st, 2011 at 14:00 local time, from Quinta Normal (33.44°S, 70.68°W, 530 m.a.s.l.) within the city of Santiago. Together with our sonde (which we call FCFM, which is the Spanish acronym for the Faculty of Physical and Mathematical Sciences) we launched two commercially available research-grade radiosondes: a Vaisala RS-92 and an InterMet iMet-1 radiosonde. The three sondes were attached to a styrofoam structure. The campaign did not proceed as originally planned because several of the sensors malfunctioned (from the commercial sondes as well as from our own sonde). Three main problems affected the development of the campaign and compromised the recovery of the sonde. First: ascent and descent velocities were computed using a payload weight of 1250 grams. This weight changed during the campaign due to extra batteries and tape being added to attach the sondes together. Therefore, the ascent velocity was smaller than calculated (~ 3 m/s instead of 5 m/s) and the descent velocity was larger than calculated (~ 4 m/s instead of 2 m/s). Second: the release did not occur at 500 hPa (~ 5.7 km), because the time condition for release was not adjusted for the small ascent rate of the balloon and because several minutes were lost during the launch procedure. Instead, the radiosonde was released at about 3.5 km above sea level. Third: we were unable to obtain a signal lock with GPS satellites with the iMet and with our sonde, likely due to interference from a nearby cell phone antenna (the Vaisala sounding system from the Chilean National Weather Service had a dedicated GPS antenna which may have made the difference.). In summary, from the three sondes, we only had a GPS signal during the ascent from the Vaisala sonde. Using the information of the actual release point, we were able to calculate a possible landing point from the WRF wind field. Since the descent velocity was incorrect due to the larger weight of the payload, the recovery team was given a possible landing point approximately 4 km south of the actual landing point. At that point, the batteries were still powering the sondes, and the team realized that the descent velocity was much larger than

312

316

320

324

328

estimated. Therefore, they decided to turn on the sonde receivers and attempt to triangulate their signals. By iterating along the path calculated by WRF and observing the strength of the signal from the receptors, they were able to determine a small section of about four blocks (within a populated part of the city) where the sonde should have landed. With no visual evidence of the sonde on the street, the team started asking people about the balloon and on the first of these attempts they found the family that recovered the sonde. Figure 4 shows the predicted and the actual trajectory followed by the sonde, as well a picture taken by the sonde near the top of the trajectory.

Figure 5 shows a portion of the data retrieved by the array of sondes. The RS92 stopped transmitting data during descent by the default configuration of the Vaisala receiving station. On the other hand the iMet radiosonde was being inadvertently interfered by another iMet radiosonde which was not the one in the array (we realized this at ~ 800 hPa into the sounding). Both the iMet and the Vaisala temperature show an almost perfect agreement between them (Fig. 5.a). The temperature from the digital sensor in our sonde suffered from a clear time lag. The time in which the sensors reached the minimum temperature is about 70 to 80 seconds longer for our digital sensor than for the research-grade radiosondes. Also, the temperature measured by our digital sensor is clearly overestimated during the ascent and underestimated during descent. This can be in part explained by the relatively large range of response-time of the sensor (see Table 1) from 8 to 30 s compared to the much faster bed thermistors used in most of the research-grade radiosondes (which have a time constant of less than one second (Nash et al. 2011)). However, most of the effect comes from a deficient design of the casing of the digital temperature/humidity sensors (see Fig. 1). Although the main purpose of the casing was to protect the sensor from direct sunlight, we inadvertently increased the stagnation of the flow around the sensor, further increasing the effective response-time in temperature. This points to the critical role of the casing design in the total error of the measurement (in this case the casing accounted for several degrees of error in temperature).

The humidity sensors, on the other hand, worked reasonably well and took measurements that were in between those of the research-grade radiosonde systems (Fig. 5.b). Vaisala humidity measurements during the ascent from the boundary layer to the free troposphere showed humidity values sharply decreasing from about 32% to less than about 8% at the top of the inversion layer. At the top of the

sounding, RH dropped to $\sim 1\%$ according to the Vaisala measurement whereas the iMet sonde registered
360 a minimum of nearly 11% and our digital and analogue RH sensors showed $\sim 6\%$ and $\sim 9\%$
respectively. Both our digital and analogue humidity sensors showed the sharp decrease of relative
humidity at the top of the boundary layer in both the ascent and the descent. Therefore, even in the
absence of the research-grade radiosonde temperature, an independent estimation of the height of the
364 boundary layer was obtained by our sonde. Again, the large response-time of our temperature sensor
filtered out all signal of the boundary layer top in our temperature profile, which is clearly visible in
both the Vaisala and iMet temperature data (Fig. 5a). There seems to be a difference in the performance
of the RH sensors between the ascent and descent which might be explained by the different velocity of
368 the sonde relative to the air, and therefore different ventilation of the payload. Also, since the digital
temperature had a time lag, the RH measured by FCFM-digital which has a temperature correction, was
also affected by the stagnation of the casing.

372 The pressure data shown in Fig. 5.c is a smoothed version of the raw pressure from the sensor using a
moving average window of 10 s. Although a calibration of the pressure was made using equipment
provided by the Chilean Meteorological Service, a small bias in pressure is observed, apparently
increasing with height. There is a small change in the pressure of the top of the mixed layer between
376 ascent and descent as observed from the horizontal line in Fig. 5.c. This may in be in part due to the
pressure bias.

380 *d. Free tropospheric sounding*

A Second campaign was carried out during May 4th 2012, at 14:00 local time to test the radiosonde
384 electronics subject to conditions in the upper troposphere as well as to test communication over a longer
range. The sonde was released at Santo Domingo (33.63°S, 71.65°W, 75 m.a.s.l) which is one of the
four official sounding stations located in Chile, and the closest to Santiago. Fig. 6 shows the comparison

between a simultaneous iMet, Vaisala and FCFM sounding. During this sounding we completely
388 removed the casing covering the digital temperature and relative humidity sensor (FCFM-Sensirion).
For this campaign we also added a new analog temperature sensor which is a thermistor that comes with
the most popular Arduino kit distribution, the “Arduino Starter Kit” (see Table 2).

392 Unfortunately, due to a bad design of the payload, we had interference between the transmitters and
the GPS receivers, so no signal from GPS was available from any of the sondes. Individually, the sondes
each obtained a GPS-signal-lock and were transmitting geolocation data to their respective receivers.
The lack of geolocation data during flight further resulted in the loss of payload after descending from
396 about 12 km (~ 220 hPa).

Despite of the loss of the payload, the radiosonde transmitted good data even during the descent.
Here, we report observations obtained from the ascent part of the sounding. There is a well mixed
400 boundary layer between surface and 970 hPa (almost constant virtual potential temperature in the layer
Fig. 6.c). Stratocumulus was present at the top of the mixed layer. There is a relatively deep temperature
inversion layer from 970 hPa to about 900 hPa. Even without the casing, the FCFM-Sensirion time lag is
long enough to smooth out the rapid change at the top of the mixed boundary layer. Fig. 6.c shows more
404 clearly the lag in temperature by the FCFM-Sensirion, nevertheless, the pressure level of the top of the
mixed boundary late could be clearly identified from our sensors. The performance of the analogue
temperature sensor was surprisingly good following very closely the behavior of the Vaisala sounding.
The mean absolute error of the temperature was about 0.85 K for the FCFM-Sensirion (mostly due to the
408 large error in temperature within the inversion layer) and only 0.4 K for the FCFM-analog. The FCFM-
Sensirion exceeded its operating range and transmitted a fixed temperature after reaching 229 K.

Both the iMet and RS-92 Vaisala show relative humidities near 100 % at the top of the mixed layer.

412 Our sensor, however, shows a $\sim 15\%$ dry bias within the mixed boundary layer (Fig. 6.b). The inversion
at the top of the well mixed boundary layer coincides with a rapid drying from near saturation at the top
of the mixed layer to about 20% RH at the top of the inversion layer (about 900 hPa). The performance
of our sensor in RH improves for drier conditions compared to Vaisala, consistent with the performance
416 during the first campaign. Near 400 hPa, there was an ice cloud which is apparently detected by the
Vaisala sounding as a thin layer of $\sim 100\%$ RH with respect to ice. In this case, both iMet and in
particular our sonde have trouble responding to the presence of the cloud, and therefore show a much
smoother curve (Vaisala sounding shows a rich structure in humidity) giving also a lower value for the
420 pressure level of the cloud. The slow time response of both iMet and FCFM-Sensirion is clearly seen in
the increase of RH above 500 hPa and also in the increase of RH from about 450 hPa to 400 hPa which
is the level of the cloud (Fig. 6).

424 Although we did not recover this first prototype of our radiosonde, the campaign was successful in
that it provided us with a wider range of atmospheric conditions to compare and to test the performance
of the sensors and the electronics. Also, we were able to receive the signal of the radiosonde over a
much longer path than previously tested (about 30 km in a direct line of sight, as calculated from the
428 balloon trajectory inferred from a WRF simulation).

4. Did Engineering students learn Meteorology by building and testing a radiosonde?

432 The main purpose of our original class was to allow students to conceive, design, implement and
operate a radiosonde. The project had an explicit engineering purpose which we believe was largely
fulfilled by most of the students. However, we also expected that as an unintended consequence of
436 building a radiosonde the students would naturally familiarize themselves with atmospheric properties

and processes. From conversations with the students at the end of the semester and from the presentations and technical reports that they handed in we can categorize the students broadly into three equally populated groups that also reflect the student interests and depth of learning:

- 440
- *Students that did not learn any meteorology.* By design of the class work, students needed to specialize in one of three tasks. The group in charge of the radiosonde communication was only barely in touch with the actual atmosphere we were planning to observe. Some of the best students
444 in the communication group however, were not in this category.
 - *Students that took meteorological observations only as a design constraint on the instruments.* At this level of learning, students were able to take into consideration the range of variables observed
448 in the real atmosphere for the selection of the sensors but did not go much further.
 - *Students that took meteorological phenomena into account for the choice of sensors and the design of the radiosonde.* These students revised the design several times in order to comply with
452 the need to observe a particular process. For instance, in order to distinguish rapid changes in the atmospheric variables with height, some students realized that there is a tradeoff between the ascent rate of the balloons (v_{asc}) and the time response of the sensors; by simply reducing the ascent rate of the balloons one is also reducing the ventilation of the sensors and therefore
456 increasing the time response. This is an important issue in the local Santiago climate where the height of the mixed boundary layer is a critical parameter for the dispersion of pollutants (e.g Muñoz and Undurraga 2010). If the depth of the inversion layer is Δh , the response time of the sensor in temperature needs to be at least $\Delta h/v_{asc}$ in order to resolve the inversion layer (this can be
460 similarly applied to the detection of a cloud layer from a RH sounding). Solving this type of problems requires the interaction between meteorologists and engineers. Other students that fall into this category were interested in knowing the height of the balloon during the trajectory. The height of the balloon was critical to our exercise as it allows for determining whether the ascent

464 and descent rates during the campaign are the ones estimated before the launching. This allows for
in-situ corrections of the radiosonde trajectory calculated from WRF. The need for the height of
the balloons led students to study the concept of geopotential height and the hydrostatic and
hypsometric equations. The idea of recovering the payload was also a motivation for some
468 students to become interested in numerical weather forecasting models, the calculation of
trajectories and the local meteorology. Several of these students have continued by enrolling in
introductory classes in meteorology.

472 Reflecting on the motivation and performance of the students during the semester, perhaps instead of
dividing the groups into particular variables to measure or parts of the radiosonde to build, it is better to
assign them to particular phenomena to observe. This puts the students in to a closer relationship with
the actual purpose of the instrument and motivates them to come back to the design of the instrument if
476 the data is not satisfactory, as opposed to students thinking that the class is over when the first prototype
is ready.

480 5. Other sensors and further development

The lessons learned from the campaigns have led to the development of many improvements to our
radiosonde system. Our first two full campaigns were successful in accomplishing some of the main
484 goals that were initially proposed to the students, namely the transmission of data during flight from
most of the depth of the troposphere, the ability to recover the radiosonde, the functioning of the
electronics subject to very cold temperatures and the ability to record and transmit data that compared
reasonably well with the operational standards.

488 Since the end of the semester, some students and most of the teaching assistants have continued
working on different aspects of the FCFM-radiosonde project. In order to improve the measurement of
humidity, we are currently developing a chilled-mirror hygrometer using Peltier cooling elements based
492 in part on the one described by Vömel et al. (2003). Control routines to sequentially cool and warm the

Peltier elements can be easily programmed to the Arduino. Also, we are attempting the integration of our system with an ozonesonde, which, being an expensive instrument to begin with (~ 1000 US\$ each ozonesonde), makes the possibility of the recovery of the ozonesonde payload much more attractive.

496 Companies that produce electrochemical ozonesondes have designed their instruments to communicate with research-grade radiosonde. Ozonesondes can be reused, provided that the reactants are replaced and the sonde is recalibrated.

500 Equally important for the continuation of the project is to improve the quality of the data obtained from the commercially available sensors, attempting to get as close as possible to the research-grade accuracy and response-time in all meteorological variables. Although our comparisons are relative to RS92 Vaisala and iMet-1 radiosondes, these instruments also suffer from biases and random errors (see
504 for instance Miloshevich et al. 2009, for a discussion of the errors in the relative humidity measurements made by the RS92 Vaisala sonde). Improvements in the data not only come from a better instrumentation but also from software corrections due to the time lag of the sensors and possibly improvements in the layout of the instruments in the payload. Attempting to solve some of these
508 challenges, make for interesting ideas for future instances of the workshop class.

If one can prove that radiosondes have errors that are smaller than operational for a significantly large number of soundings, the idea of adaptive sounding as proposed by Douglas (2010) becomes
512 feasible using our system, given the relatively low cost of implementation of a ground receiving station (the limiting issue then becoming the availability of gas supply). Although the cost of our radiosonde turned out to be of the order of the current commercial radiosondes, the receiver (ground station) is several orders of magnitude cheaper than commercial solutions. In addition to this, the cost of the
516 radiosonde can be of less relevance if we notice two extra advantages of developing a reusable radiosonde, specially as an open software/hardware initiative: 1) open initiatives tend to be developed

faster than closed ones due to the community cooperation and 2) specific needs (e.g., radio observatories needing very accurate humidity measurements in the upper troposphere to perform interferometry observations) can be addressed by adding new custom made sensors in a much easier and flexible manner.

Other improvements to the system involve the visualization and trajectory software to allow for the real-time correction of the forecast trajectory of the radiosonde to speed up the recovery of the radiosonde package. Also, the Arduino board can be programmed so that in the case of encountering interference at the ground or during the trajectory, the GPS module can be reinitialized and the GPS signal-lock can be recovered. Nevertheless, the successful recovery of the payload requires not only having the technology in place, but also a strict set of protocols to be followed by the people participating in the campaign (something that mission planning engineers must know now for decades).

From a pedagogical point of view we believe that this exercise is beneficial for both meteorologists and engineers. Meteorologists get a first hand sense of the data they analyze and study; they recognize the source of errors by looking at amplified versions of the errors relative to what they will encounter in the commercial radiosondes. Engineers on the other hand learn meteorology (even sometimes inadvertently) by attempting to solve seemingly practical problems. In retrospect, the greatest change we would make to future instances of the class, it would be to focusing the main objective of the class from the beginning on measuring particular meteorological phenomena rather in the construction and integration of the parts and pieces of the equipment.

We have developed a website (<http://www.dgf.uchile.cl/radiosonde>) which provides the details of the construction, parts and programming involved in the radiosonde, so we hope several others will attempt the construction of the radiosonde either as a part of the regular curriculum of engineering and meteorology or simply by enthusiasm. If a community of users and developers flourishes, we hope that

many unexpected improvements of the platform that we present here will ensue.

544 ***Acknowledgments.***

548 *We appreciate the help of the Chilean National Weather Service (Dirección Meteorológica de Chile, DMC) for providing access to an environmental chamber to make the calibration of our sensors, and also for providing the ground stations for retrieving the Vaisala measurements. We thank comments and suggestions by three anonymous reviewers and also by Dr. Ricardo Muñoz that significantly improved the original manuscript.*

552

References

- 556 Assman, R., 1902: Über die existenz eines wärmeren luftstromes in der höhe von 10 bis 15km. *Sitzber. Konigl. Preuss. Akad. Wiss. Berlin*, **24**, 495–504.
- 560 Clayton, H. H. and S. P. Fergusson, 1909: Exploration of the upper air by means of ballons-sondes, at St. Louis, in the years 1904 - 07. *Annals of Harvard College Observatory*, **68**.
- 564 Crawley, E., J. Malmqvist, and S. Östlund, 2007: *Rethinking engineering education: The CDIO approach*, Vol. 133. Springer Verlag.
- 568 Dabberdt, W., H. Cole, A. Paukkunen, J. Horhammer, V. Antikainen, and R. Shellhorn, 2002: *Radiosondes*, Vol. 6, 1900–1913. Academic Press, San Diego.
- Douglas, M., 2010: Adaptive sounding arrays for tropical regions. *29th Conference on Hurricanes and*
- 572 *Tropical Meteorology*, American Meteorological Society.
- DuBois, J., R. Multhauf, and C. Ziegler, 2002: *The Invention and Development of the Radiosonde with a*
- Catalog of Upper-Atmospheric Telemetering Probes in the National Museum of American History*,
- 576 *Smithsonian Institution*. No. 53 in *Smithsonian studies in history and technology*, Smithsonian Institution Press, Washington, D.C.
- Hergesell, H., 1906: Ballon-Aufstiege über dem freien Meere zur Erfassung der Temperatur- und
- 580 Feuchtigkeitsverhältnisse sowie der Luftströmungen bis zu sehr grossen Höhen der Atmosphäre. *Beitr. z. Phys. d. fr. Atm*, **1**, 200–204.
- 584 Immler, F., J. Dykema, T. Gardiner, D. Whiteman, P. Thorne, and H. Vömel, 2010: Reference Quality Upper-Air Measurements: guidance for developing GRUAN data products. *Atmospheric Measurement Techniques*, **3**, 1217–1231.
- 588 Miloshevich, L., H. Vömel, D. Whiteman, and T. Leblanc, 2009: Accuracy assessment and correction of Vaisala RS92 radiosonde water vapor measurements. *J. Geophys. Res*, **114**, D11 305.

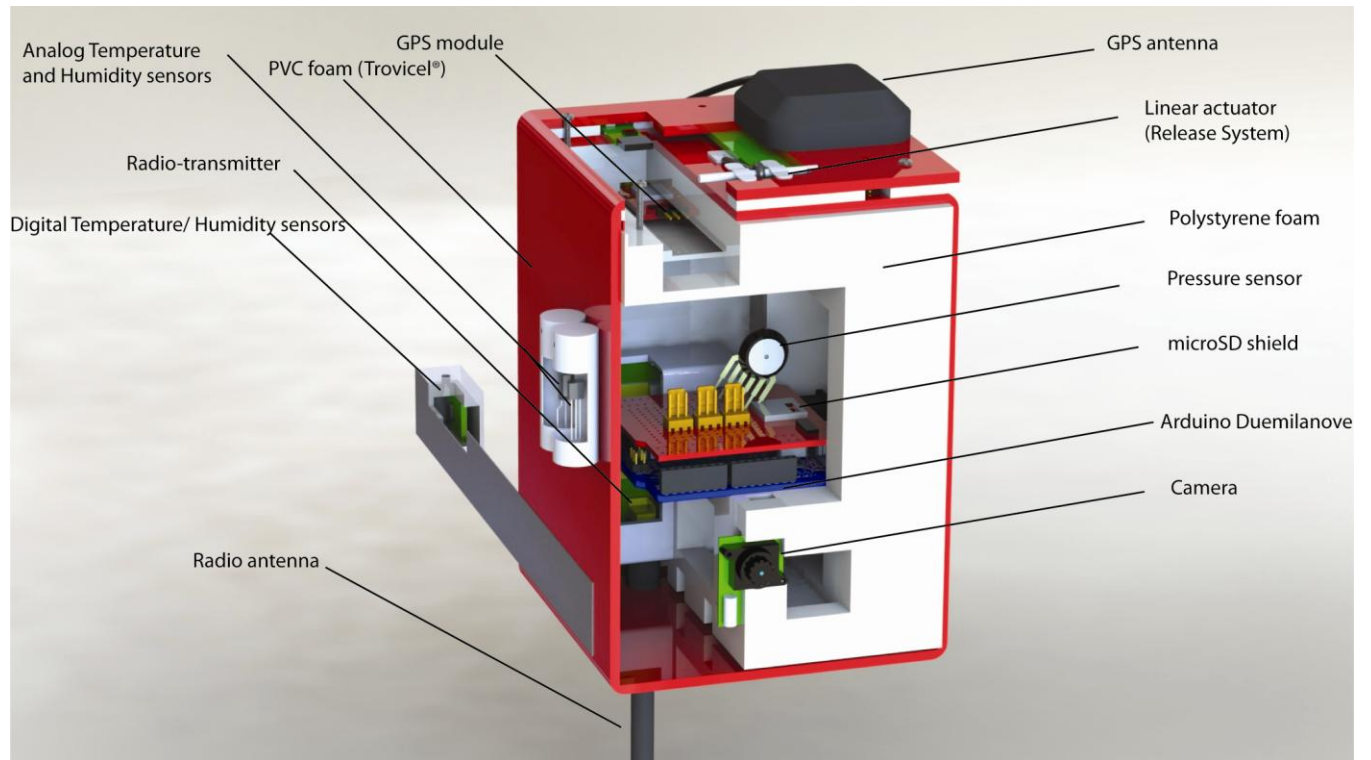
- Muñoz, R. and A. Undurraga, 2010: Daytime mixed layer over the santiago basin: Description of
 592 two years of observations with a lidar ceilometer. *Journal of Applied Meteorology and Climatology*,
 49, 1728–1741.
- Nash, J., T. Oakley, H. Vömel, and L. Wei, 2011: WMO intercomparison of high quality radiosonde
 systems, Yangjian China, 12th July to 3rd August. Tech. rep., World Meteorological Organization.
- 596 Pettifer, R., 2009: From observations to forecasts-part 2. The development of in situ upper air
 measurements. *Weather*, **64 (11)**, 302–308.
- 600 Sarik, J. and I. Kymissis, 2010: *Lab kits using the Arduino prototyping platform*, T3C–1. 40th
 ASEE/IEEE Frontiers in Education Conference, IEEE.
- Skamarock, W., J. Klemp, J. Dudhia, D. Gill, D. Barker, W. Wang, and J. Powers, 2008: A Description of
 604 the Advanced Research WRF Version 3. Tech. rep., NCAR. NCAR Tech Notes-475+ STR.
- Teisserenc de Bort, L., 1902: Variations de la température de l'air libre dans la zona comprise entre 8km
 et 13km d'altitude. *Comptes Rendus de l'Acad. Sci. Paris*, **134 (987.989)**.
- 608 Thorne, P., J. Lanzante, T. Peterson, D. Seidel, and K. Shine, 2011: Tropospheric temperature trends:
 history of an ongoing controversy. *Wiley Interdisciplinary Reviews: Climate Change*, **2 (1)**, 66–88.
- 612 Vömel, H., M. Fujiwara, M. Shiotani, F. Hasebe, S. Oltmans, and J. Barnes, 2003: The behavior of the
 snow white chilled-mirror hygrometer in extremely dry conditions. *Journal of Atmospheric and Oceanic
 Technology*, **20 (11)**, 1560–1567.

616

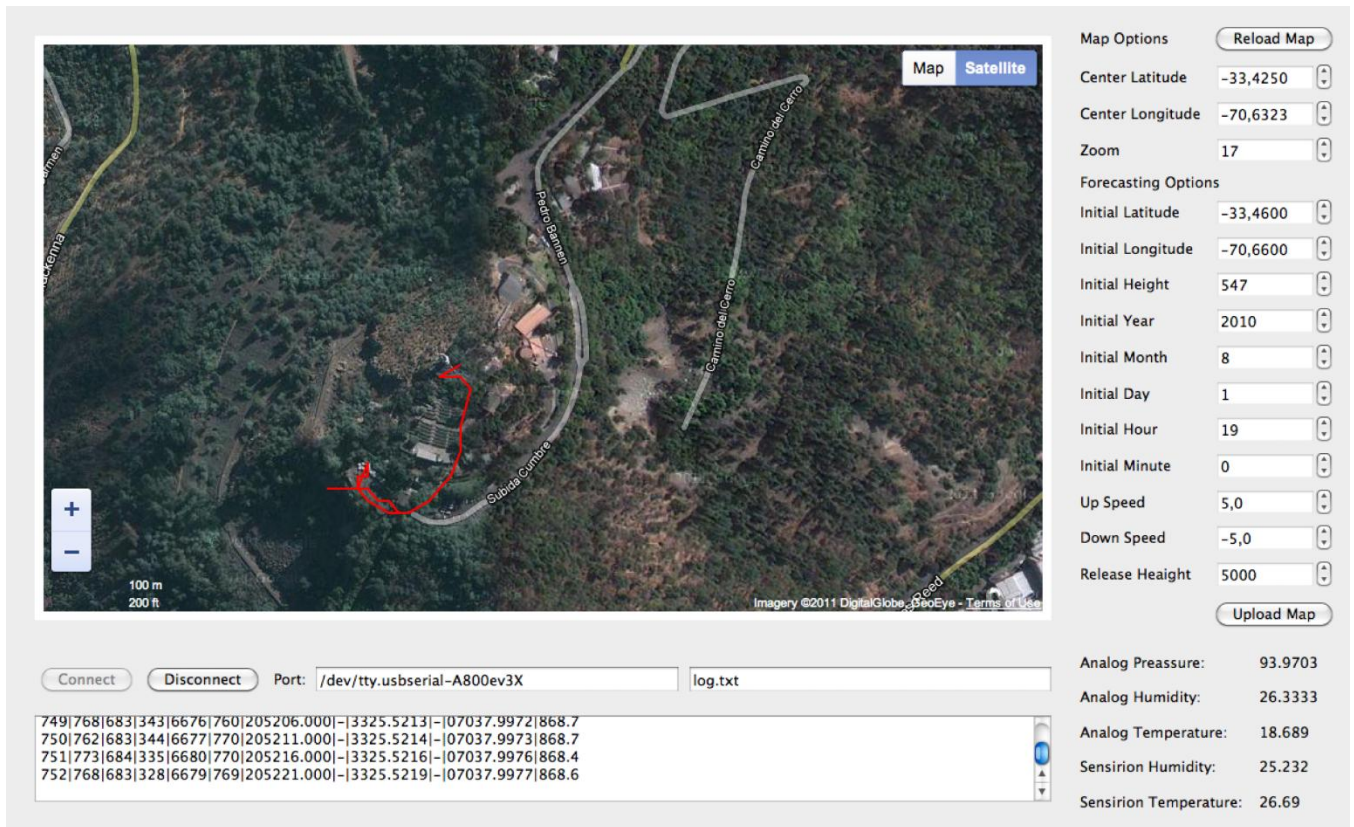
620

List of Figures

624	Figure 1 Cut-away view of the radiosonde, showing the parts and sensors.	23
628	Figure 2 Screenshot of the BaseCamp software showing the trajectory followed by the students around top of the San Cristobal hill in downtown Santiago. The data was received by students located on the roof of the Geophysics building about 4 km line-of-sight from the top of the hill.	24
632	Figure 3 WRF calculated trajectories (open circles) and actual observed trajectories (closed circles) for three consecutive days (16, 17 and 18 May 2011 at 14:00 local time). The observed trajectories are the trajectories followed by the radiosondes launched from Quinta Normal station in Santiago. The colorbar indicates height above Santiago (in meters). Taking as a reference the Andes piedmont, which nearly coincides with the bounds of the city of Santiago, the trajectories show good agreement (within 5 km to the real ones) for the first 10 km in height, even though they show a separation of about 30 km from one day to the next for this particular case. White segments joining the calculated and real sonde trajectories are about 5 km in length. Several trajectories were calculated from WRF output in a similar fashion for dates in which soundings starting at the main office of the Chilean National Weather Service in Santiago were available, and they all showed a similar agreement.	25
640	Figure 4 Aerial view showing the predicted (yellow) and actual trajectory (red) of the radiosonde during the ascent and descent for the Santiago campaign. The missing GPS data of the descent is represented with dashed lines. The forecast trajectory was made a-posteriori, knowing the exact ascent and descent velocities. The forecast was made 24 hours before the launch. The separation between the end of the forecast trajectory and the actual landing point was about 700 m. Images in panels (a) and (b) were modified from Google Earth. Panel (c) shows a picture taken by the radiosonde near the top of the sounding and looking in the direction marked by the white arrow in panel (b).	26
648	Figure 5 The panels show time series data of the different meteorological sensors from the three different sondes during the boundary layer intercomparison campaign. The three sondes are referred to as FCFM, Vaisala RS92 and iMet. a) Temperature, b) Relative Humidity and c) Pressure. The light blue dashed lines show the approximate time at which the sonde crossed the top of the boundary layer during the ascent and descent. The horizontal light blue line shows the estimated pressure of the top of the boundary layer.	27
652	Figure 6 The panels show ascent vertical profiles for the free troposphere intercomparison campaign of May 4th 2012. (a) Temperature in Kelvin degrees as a function of pressure. (b) Relative Humidity and (c) A view of the boundary layer virtual potential temperature.	28
660		

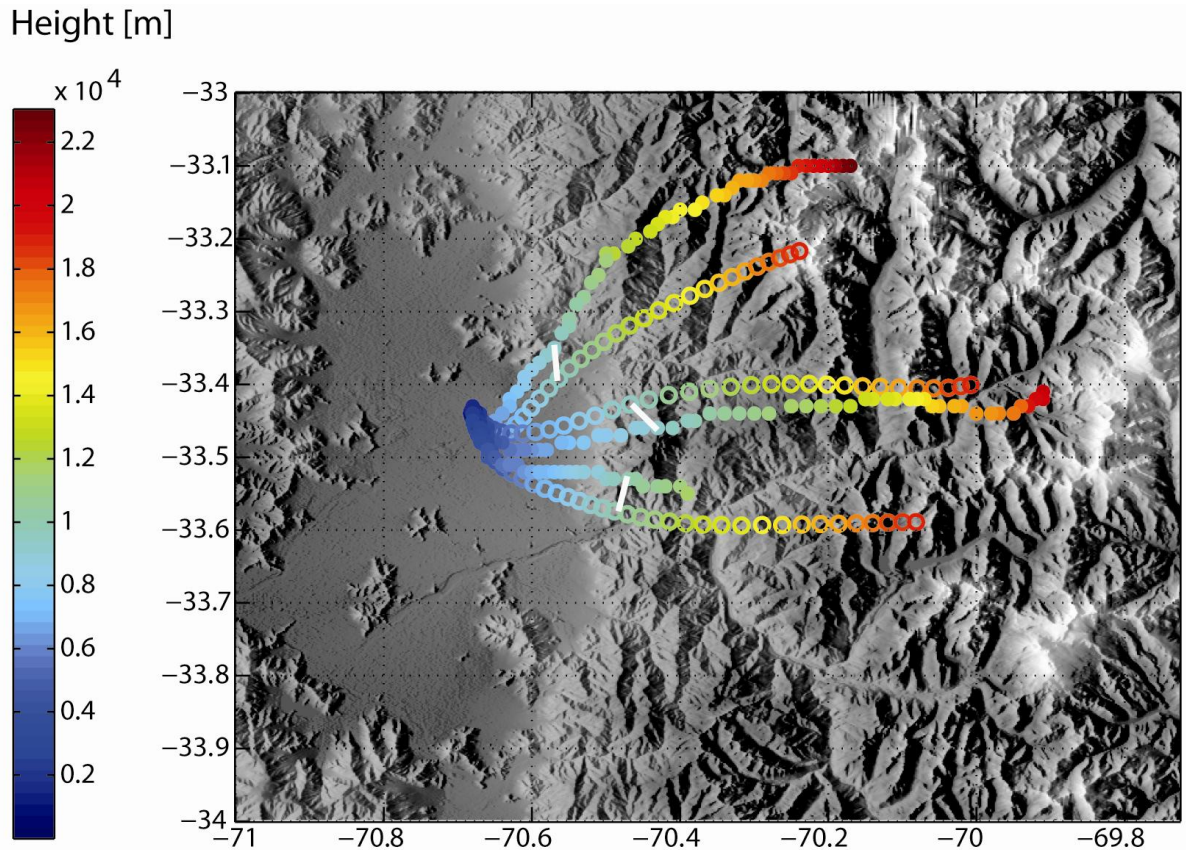


664 **Figure 1** Cut-away view of the radiosonde, showing the parts and sensors.

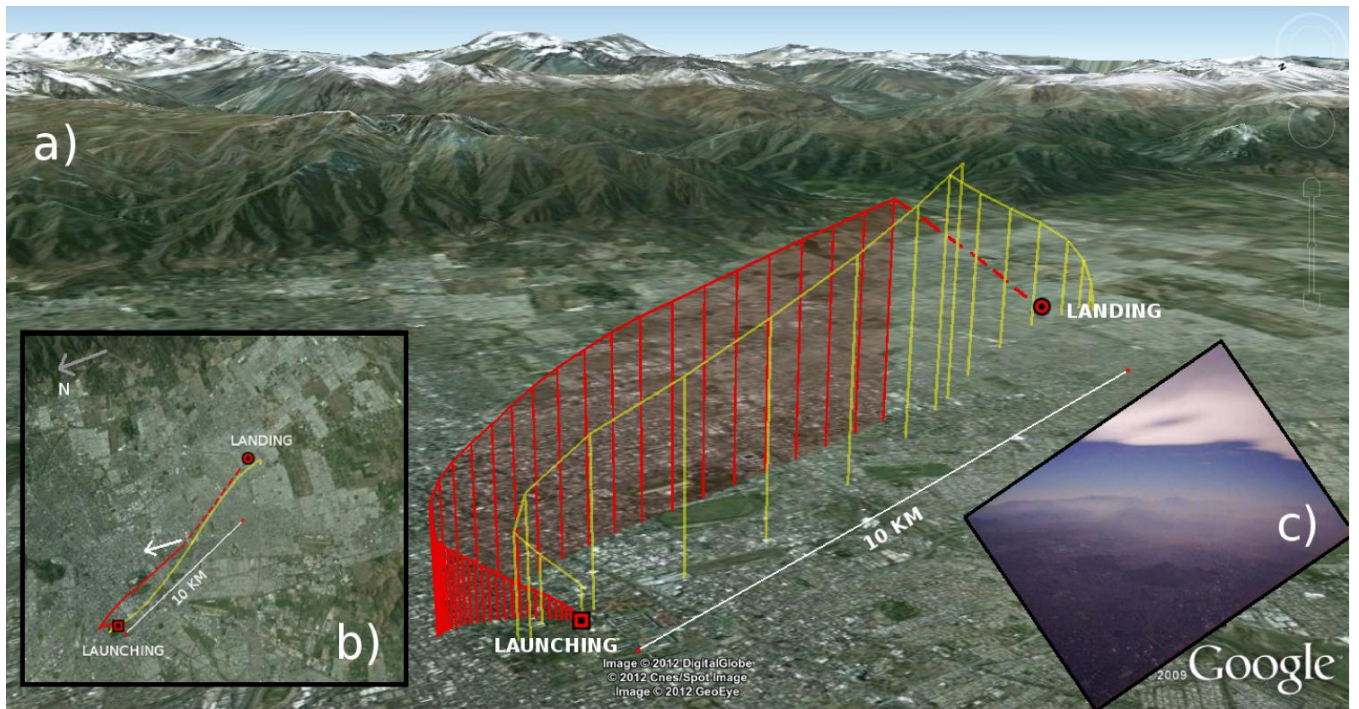


668 **Figure 2 Screenshot of the BaseCamp software showing the trajectory followed by the students around top of the San Cristobal hill in downtown Santiago. The data was received by students located on the roof of the Geophysics building about 4 km line-of-sight from the top of the hill.**

672



676 **Figure 3** WRF calculated trajectories (open circles) and actual observed trajectories (closed
 680 circles) for three consecutive days (16, 17 and 18 May 2011 at 14:00 local time). The observed
 trajectories are the trajectories followed by the radiosondes launched from Quinta Normal station
 in Santiago. The colorbar indicates height above Santiago (in meters). Taking as a reference the
 684 Andes piedmont, which nearly coincides with the bounds of the city of Santiago, the trajectories
 show good agreement (within 5 km to the real ones) for the first 10 km in height, even though they
 show a separation of about 30 km from one day to the next for this particular case. White
 segments joining the calculated and real sonde trajectories are about 5 km in length. Several
 trajectories were calculated from WRF output in a similar fashion for dates in which soundings
 starting at the main office of the Chilean National Weather Service in Santiago were available,
 and they all showed a similar agreement.

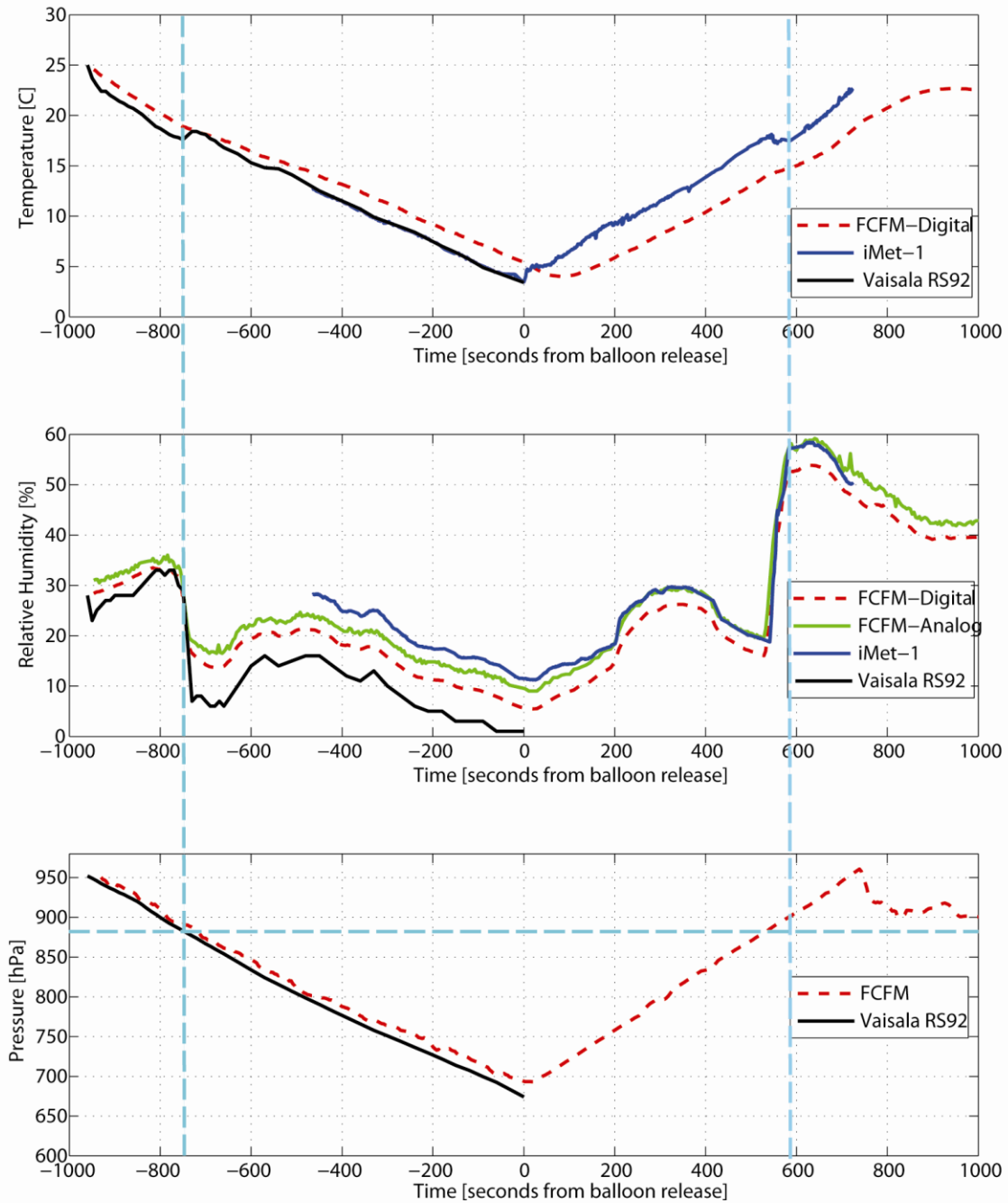


688

692

696

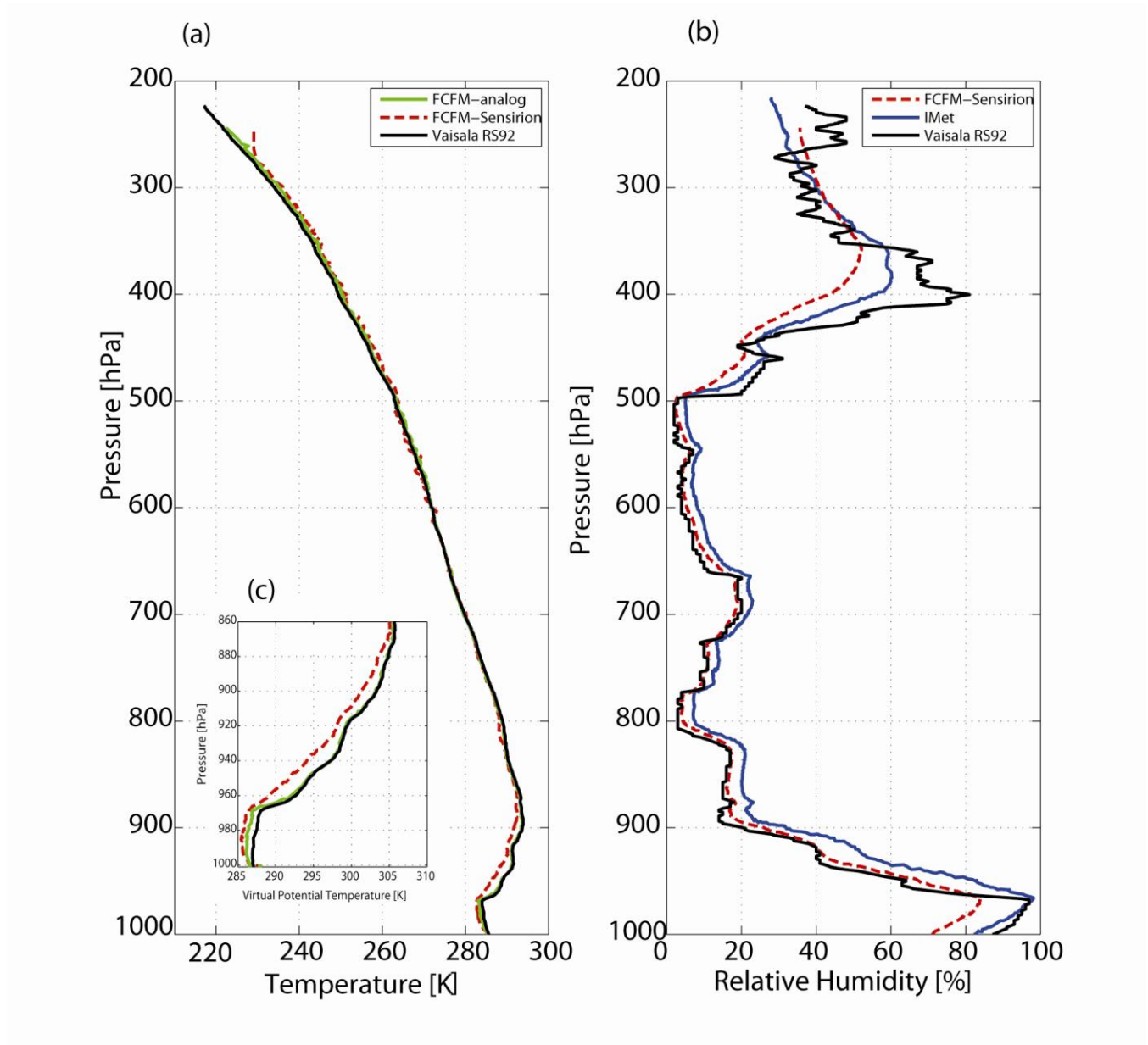
Figure 4 Aerial view showing the predicted (yellow) and actual trajectory (red) of the radiosonde during the ascent and descent for the Santiago campaign. The missing GPS data of the descent is represented with dashed lines. The forecast trajectory was made a-posteriori, knowing the exact ascent and descent velocities. The forecast was made 24 hours before the launch. The separation between the end of the forecast trajectory and the actual landing point was about 700 m. Images in panels (a) and (b) were modified from Google Earth. Panel (c) shows a picture taken by the radiosonde near the top of the sounding and looking in the direction marked by the white arrow in panel (b).



700

704

Figure 5 The panels show time series data of the different meteorological sensors from the three different sondes during the boundary layer intercomparison campaign. The three sondes are referred to as FCFM, Vaisala RS92 and iMet. a) Temperature, b) Relative Humidity and c) Pressure. The light blue dashed lines show the approximate time at which the sonde crossed the top of the boundary layer during the ascent and descent. The horizontal light blue line shows the estimated pressure of the top of the boundary layer.



708

Figure 6 The panels show ascent vertical profiles for the free troposphere intercomparison campaign of May 4th 2012. (a) Temperature in Kelvin degrees as a function of pressure. (b) Relative Humidity and (c) A view of the boundary layer virtual potential temperature.

712

716

Engineering Specialty	Radiosonde building and calibration	Sounding
Computer Science	<ul style="list-style-type: none"> • Programming of the microcontroller. • Development of the communication protocols for the radiotransmission. 	<ul style="list-style-type: none"> • Estimation of the wind from the GPS position. • Development of a Graphic User Interface.
Chemistry/ Chemical Engineering	<ul style="list-style-type: none"> • Design and construction of the insulation for the electronics to prevent malfunction of the components at very low temperatures of high humidity. • Calibration of RH using air in equilibrium with chemical solutions. 	<ul style="list-style-type: none"> • The resistance of the balloon material and the thermodynamics of the sounding determine the burst height and the final diameter of the balloon.
Electrical/ Electronic	<ul style="list-style-type: none"> • Integration of the sensors with the microcontroller • Estimation of the power consumption of the elements in the radiosonde • Development of the communication protocols for the radiotransmission 	<ul style="list-style-type: none"> • Design of antennas to allow for a larger range of data reception • Layout of electronics to avoid interference of the data stream and the GPS signal.
Mechanical/Aerospace	<ul style="list-style-type: none"> • Design of an automatic release system for recovery of the payload. 	<ul style="list-style-type: none"> • Calculation of the balloon aerodynamics which determines the rate of ascent and initial filling of the balloons.
Industrial	<ul style="list-style-type: none"> • Estimation of the costs and management of the project. 	<ul style="list-style-type: none"> • Development of launching mission protocols.

720 **Table 1** Some individual tasks carried out during construction, calibration and operation of the radiosonde

Name	Description	Part Number	Vendor/ Manufacturer	Variable / Function	Measuring/ Operating Range	Error	Response time / Sampling Frequency	Value
Analogue Temperature Sensor	10 k Thermistor	2322 640	Olimex/ Vishay BC- components	Temperature	-40 to 125 C	~ 1 C	15 s	US\$ 2.0
Analogue Temperature Sensor	2-terminal zener with voltage proportional to temperature	LM235Z	Digikey/ National Semiconductor Corporation	Temperature	-40 to 125 C	1 C	3 s (@ 5 m/s)	US\$ 1.5
Analogue Humidity Sensor	Thermoset polymer capacitive sensing element	HIH-4010-001	Digikey/ Honeywell	Relative Humidity	0-100 % RH	± 3.5 %	5 s (slow moving air)	US\$20
Analogue Pressure Sensor	Integrated silicon piezoresistive transducer with analogue output	MPX5100D	Digikey / Motorola	Pressure	0-1000 hPa	± 25 hPa	1 ms	US\$16
Humidity and temperature digital sensor	Capacitive sensor (RH) Band Gap sensor (Temperature)	SHT10	Sensirion	Humidity Temperature	0-100 % RH -40 to 124 C	± 4.5 % ± 0.5 C	8 s 5 to 30 s	US\$ 15
GPS Module / Current	GPS Sirf Star III module with internal patch antenna	MOD-GPS	Olimex	Wind, Position	-40 to 85 C (< 18 km height)	1 - 3 m/s (at 10 m/s)	< 1 s	US \$ 50
GPS Module / Discontinued	SparkFun GPS micro-mini	MN5010HS	SparkFun	Wind, Position	-20 to 85 C (< 18 km height)	≤ 3 m	< 1 s	
Communication transceiver	Data radio module	HAC-LM12	Shenzen HAC Technology	Radio transmission	402-405 Mhz			US\$ 50
Camera / Discontinued	VGA module	C328-7640	COMedia Ltd	Image Capture			5 minutes	US\$ 39
Linear Actuator	MigaOne-12 Linear actuator		Miga Motor Company	Release System				US\$ 40
Switch	Miga Analog Driver V5		Miga Motor Company	Release System				US\$ 14
Microcontroller	Arduino Uno	DEV-10356	SparkFun	Radiosonde brain				US\$ 30
Board	MicroSD Arduino Shield PCB	DEV-09802	SparkFun	Radiosonde sensors board				US\$ 15
Battery	Polymer Lithium Ion Battery 1000mAh 7.4 V	PRT-10472	SparkFun / King Max					US\$ 7

Table 2 Parts, pieces and sensors used in building the radiosonde. Prices are in the US without taxes or shipping.